

Possibility of an adiabatic transport of an edge Majorana through an extended gapless region

Atanu Rajak,¹ Tanay Nag,² and Amit Dutta²

¹*Saha Institute of Nuclear Physics, 1/AF Bidhannagar, Kolkata 700 064, India*

²*Indian Institute of Technology Kanpur, Kanpur 208 016, India*

In the context of slow quenching dynamics of a p -wave superconducting chain, it has been shown that a Majorana edge state can not be adiabatically transported from one topological phase to the other separated by a quantum critical line. On the other hand, the inclusion of a phase factor in the hopping term, that breaks the effective time reversal invariance, results in an extended gapless region between two topological phases. We show that for a finite chain with an open boundary condition there exists a non-zero probability that an edge Majorana can be adiabatically transported from one topological phase to the other across this gapless region following a slow quench of the superconducting term; this happens for an optimum transit time, that is proportional to the system size and diverges for a thermodynamically large chain. We attribute this phenomenon to the mixing of the Majorana only with low-lying inverted bulk states. Remarkably, the Majorana state always persists with the same probability even after the quenching is stopped. For a periodic chain, on the other hand, we find a Kibble-Zurek scaling of the defect density with a renormalized rate of quenching.

PACS numbers: 74.40.Kb, 74.40.Gh, 75.10.Pq

I. INTRODUCTION

The p -wave superconducting chain, introduced by Kitaev [1] has become a topic of immense interest in recent years for its fascinating topological properties [2–7]. These studies lie at the interface of condensed matter physics, quantum information processing, decoherence and quantum computation [8–10]. The remarkable property of the model is that the topological phase hosts zero energy Majorana modes at the ends of an open chain as the midgap excitations between positive and negative energy bulk states; a topological phase is separated by a quantum critical line from the other topological and non-topological phases as also happens in a topological insulators [11, 12]. It has been proposed that Majorana states can possibly be achieved by the proximity effect between the surface state of a strong topological insulator and a s -wave superconductor [13]. The experimental realization of the zero-energy Majorana modes have been found recently in nanowires coupled to superconductors [14–18]; these experimental observations however are challenged theoretically [19]. The hybridization of Majorana fermions has also been observed experimentally through the zero-bias anomalies in the differential conductance of an InAs nanowire coupled to superconductor [20].

On the other hand, given the recent interest in the non-equilibrium quenching dynamics of quantum many body systems across quantum critical points (QCPs) (for review articles see [21–23]), the studies involving quenching dynamics of a topological system across a QCP [24–26] have emerged as a rapidly growing field of research. Especially, the quenching dynamics of a topological insulator [27] and the p -wave superconducting chain [28–30] have been explored in this connection. We note that the dynamical generation[31], formation and manipulation[32] of edge Majorana states for a driven system have also

been studied extensively.

Bermudez *et al.* [25], addressed the question whether an adiabatic transport of an initial edge Majorana state from one topological phase to the other is possible when the hopping amplitude of the p -wave superconducting Hamiltonian is slowly varied in a linear fashion with time. It has been found that such an adiabatic transportation of edge Majorana is forbidden as it gets completely delocalized throughout the chain when the system reaches the QCP separating the two topological phases.

We here consider a modified p -wave superconducting chain with a complex hopping term which breaks the effective time reversal symmetry (ETRS) of the model as well as generates an extended gapless phase separating two topological phases as introduced in Ref. 7. In this communication, we probe the question of transporting an edge Majorana adiabatically from one topological phase to the other for a finite chain which is driven across this extended quantum critical region. Our most significant observation is that indeed there exists a finite probability for Majorana edge state, to tunnel adiabatically through the intermediate gapless region when the superconducting gap parameter is tuned in a linear fashion with a finite quenching rate. The non-zero value of the modulus square of the overlap between the final state reached after the quenching and the equilibrium Majorana state in the other topological phase provides a measure of finding an adiabatically transported edge Majorana. We also argue that the final time-evolved edge Majorana state is not instantaneous rather persists perpetually even when the quenching is stopped. We emphasize at the outset that this adiabatic transport is only possible for an optimal transit time that the system requires to traverse the gapless region. To the best of our knowledge, our work is the first one which points to the possibility of the adiabatic passage of an edge Majorana from one phase to the other

under a slow quenching of a finite Majorana chain.

The paper is organized in the following way: in Sec. II, we describe the model Hamiltonian with the equilibrium phase diagram showing different topologically trivial and non-trivial phases. The quenching dynamics of the model with a periodic boundary condition (PBC) is studied in Sec. III, where we show that the defect density satisfies the Kibble-Zurek scaling relation with a renormalized rate of quenching. On the other hand, in Sec. IV we study the dynamics of the Majorana chain with an open boundary condition (OBC) and discuss the possibility of the adiabatic transport of edge Majorana from one topological phase to the other across the gapless phase. We make the concluding remarks in Sec. V. Finally, three Appendices have been added which to supplement the results and analysis presented in the body of the work.

II. MODEL AND PHASE DIAGRAM

The model we consider here is defined by the Hamiltonian of a 1D p -wave superconductor with a complex hopping term [6]

$$H = \sum_{n=1}^{N-1} \left[-w_0 e^{i\phi} f_n^\dagger f_{n+1} - w_0 e^{-i\phi} f_{n+1}^\dagger f_n + \Delta(f_n f_{n+1} + f_{n+1}^\dagger f_n^\dagger) \right] - \sum_{n=1}^N \mu(f_n^\dagger f_n - 1/2), \quad (1)$$

where w_0 , ϕ , Δ and μ are nearest-neighbor hopping amplitude, phase of the hopping term, superconducting gap and chemical potential, respectively with N being the number of lattice sites. The annihilation and creation operators f_n (f_n^\dagger), defined at the lattice site n , satisfy the fermionic anti-commutation relations $\{f_m, f_n\} = 0$ and $\{f_m, f_n^\dagger\} = \delta_{mn}$.

The Hamiltonian (1) can then be diagonalized in the Fourier space under PBC and is given by

$$h_k = (2w_0 \sin \phi \sin k) I - (2w_0 \cos \phi \cos k + \mu) \sigma^z + (2\Delta \sin k) \sigma^y, \quad (2)$$

where σ^y and σ^z are Pauli matrices in particle-hole subspace. (Note that $h_{-k}^* \neq h_k$ except $\phi = 0$ or π which implies the breaking of ETRS.) One can locate the QCPs associated with the Hamiltonian (2) when the bulk energy gap vanishes for the critical modes k_c ; this happens when the parameters satisfy the condition:

$$(2w_0 \cos \phi \cos k_c + \mu)^2 + 4\Delta^2 \sin^2 k_c = 4w_0^2 \sin^2 \phi \sin^2 k_c. \quad (3)$$

The phase diagrams of the model for different $\phi \in [0, \pi/2]$, obtained by analyzing the spectrum are shown in the Fig. (1). The shaded region of the phase diagram representing the gapless region is bounded by a rectangular region encapped by two elliptical arcs both in left and right sides of the rectangle (except for the

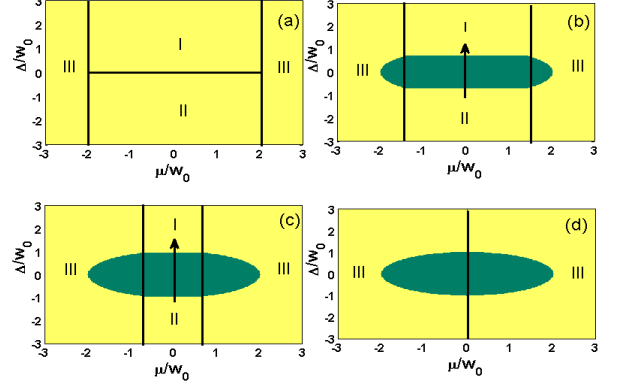


FIG. 1: (Color online) Phase diagram of the Model Hamiltonian (1) for different phases of hopping parameter (a) $\phi = 0$, (b) $\phi = \pi/4$, (c) $\phi = 2\pi/5$ and (d) $\phi = \pi/2$. Here, I and II are two distinct topological phases and III is the non-topological phase. The quenching path is shown using the vertical arrow.

special cases with $\phi = 0$ and $\pi/2$). The two sides of the rectangle in Fig. (1) are bounded by the horizontal lines $\Delta/w_0 = \pm \sin \phi$ whereas the vertical edges are given by $\mu/w_0 = \pm 2 \cos \phi$. As ϕ increases, two vertical phase boundaries approach closer and combine at $\mu = 0$ for $\phi = \pi/2$ when the topological phases disappear completely and the gapless region is bounded by an ellipse described by $\mu^2 + 4\Delta^2 = 4w_0^2$.

In order to explore the topological properties of the model, we use a real space representation of an open chain Hamiltonian (1) in terms of the two Majorana operators a_n and b_n at each site are defined as

$$f_n = \frac{1}{2} (a_n + ib_n), \quad f_n^\dagger = \frac{1}{2} (a_n - ib_n), \quad (4)$$

where a_n and b_n are real and Hermitian and satisfy the relations $\{a_m, a_n\} = \{b_m, b_n\} = 2\delta_{mn}$ and $\{a_m, b_n\} = 0$. This allows us to write the Hamiltonian with an open boundary condition in the following form

$$H = -\frac{i}{2} \sum_{n=1}^{N-1} \left[w_0 \cos \phi (a_n b_{n+1} + a_n b_{n-1}) - \Delta (a_n b_{n+1} - a_n b_{n-1}) + w_0 \sin \phi (a_n a_{n+1} + b_n b_{n+1}) \right] - \frac{i}{2} \sum_{n=1}^N \mu a_n b_n. \quad (5)$$

The Hamiltonian (5) exhibits a conspicuous band inversion phenomena near zero energy levels within the region bounded by $\Delta/w_0 = -\sin \phi$ and $\Delta/w_0 = \sin \phi$; for the detailed analysis of the spectrum see the Appendix A. Furthermore, for any non-zero value of ϕ the Majorana modes a_n and b_n can not be decoupled. We note that for $\phi = 0$, the topological phase I (phase II) is characterized by the presence of an isolated zero-energy Majorana

mode $a_1(b_1)$ at the left edge and $b_N(a_N)$ at right edge when $\Delta = w_0$ and $\mu = 0$. We set $w_0 = 1$ for the rest of the paper.

III. QUENCHING DYNAMICS OF THE PERIODIC CHAIN

In this section, we will study the quenching dynamics of the Hamiltonian (1) of the main text with a periodic boundary condition (when the Majorana edge states do not exist) choosing a linear time variation of the superconducting term of the form $\Delta(t) = -1 + 2t/\tau$, where $\tau (\gg 1)$ is the inverse of quenching rate and time t runs from 0 to τ ; without any loss of generality, we shall choose the path $\mu/w_0 = 0$. As a result, the system is quenched from phase II to phase I in Fig. (1) through the gapless region. The vertical span of the gapless region is maximum for the chosen path.

The quenching dynamics through an extended gapless phase leads to some interesting observations (e.g., exponentially decaying defect density with quenching rate) which have studied extensively [33]. Here, we shall estimate the defect density as a function of τ and ϕ following the above mentioned adiabatic quench through the extended gapless region.

In momentum space, the Hamiltonian (1) gets decoupled to different k -modes: $H = \sum_{k=0}^{\pi} h_k$ with h_k being a 2×2 matrix (2) of the main text; the reduced 2×2 space spanned by the basis vectors $|0\rangle$ (with no quasi-particle) and $|k, -k\rangle$ (with quasi-particles having opposite momenta k and $-k$). Along the chosen quenching path $\mu = 0$, there exist a finite number of degenerate critical momentum modes for which energy gap vanishes within the gapless region with $k_c = \sin^{-1}(\pm \cos \phi / \sqrt{1 - \Delta^2})$. For the positive interval lying between $0 < k_c < \pi$, these modes are ranging symmetrically around $k_c = \pi/2$ (critical mode at the boundary of the gapless region $\Delta = \pm \sin \phi$) starting from a degenerate critical mode $k_c = \pi/2 + \phi$ (critical mode at the center of the gapless region $\Delta = 0$) to the other degenerate critical mode $k_c = \pi/2 - \phi$ (critical mode at the center of the gapless region $\Delta = 0$); same as the negative side of the interval lying between $-\pi < k_c < 0$ where $k_c = -\pi/2$ is the central critical mode. To derive the scaling of the defect density, we shall make resort to the Landau-Zener (LZ) transition formula[34]; following an appropriate unitary transformation we can re-write the 2×2 matrix h_k as

$$h_k(t) = (2 \sin \phi \sin k) I + (2\Delta(t) \sin k) \sigma^z + (2 \cos \phi \cos k) \sigma^y \quad (6)$$

where the time dependent parameter $\Delta(t)$ is shifted to the diagonal.

The time evolution of the system under the above mentioned quenching scheme is governed by the time dependent Schrödinger equation

$$i \frac{\partial |\psi_k(t)\rangle}{\partial t} = h_k |\psi_k(t)\rangle, \quad (7)$$

where at any instant t , the state $|\psi_k(t)\rangle$ can be written as $|\psi_k(t)\rangle = u_k(t)|1_k\rangle + v_k(t)|2_k\rangle$, where $u_k(t)$ and $v_k(t)$ are time-dependent amplitudes and we have chosen the initial condition: $u_k(0) = 1$ and $v_k(0) = 0$. The point to note here that $|1_k\rangle$ and $|2_k\rangle$ can be written as a linear combination of $|0\rangle$ and $|k, -k\rangle$.

The above Schrödinger equation can be solved analytically for each momentum mode and an exact form of excitation probability (p_k) at final time ($t \rightarrow \infty$) can be obtained using the LZ non-adiabatic transition probability. The Hamiltonian (6) consists of two parts: the term with the identity operator that does not play any role in time evolution (though essential to achieve the extended gapless region) while the dynamics is dictated by the 2×2 LZ term. One can then readily obtain the probability of defect at the final state for each mode [35]

$$p_k = e^{-2\pi\gamma_k}, \quad (8)$$

where $\gamma_k = \delta_k^2 / |\frac{d}{dt}(E_1 - E_2)|$, $\delta_k = 2 \cos \phi \cos k$ and $E_{1,2} = \pm 2\Delta(t) \sin k$. In the thermodynamic limit, one can calculate the defect density by integrating the p_k over the k modes lying within the 1st Brillouin zone

$$n = \frac{2\pi}{N} \int_{-\pi}^{\pi} p_k dk \sim \frac{1}{\pi} \frac{1}{\cos \phi \sqrt{\tau}} \sim \frac{1}{\pi \sqrt{\tau}} \frac{1}{\sqrt{1 - W_d^2/4}}. \quad (9)$$

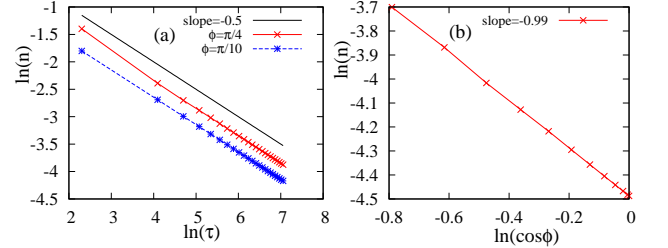


FIG. 2: (Color online) (a) The logarithm of defect density $\ln n$ with the logarithm of quench time $\ln \tau$ for $\phi = \pi/4$ and $\pi/10$ are plotted. (b) The plot shows the variation of $\ln n$ with $\ln \cos \phi$ for a quench time $\tau = 200$ which confirms the ϕ dependence of n given in Eq. (9).

In deriving the above relation, one has to use the fact that the maximum contribution to the defect comes from the modes close to the “critical” mode, for which the gap vanishes for the LZ part, $\sim \sqrt{\Delta^2 \sin^2 k + \cos^2 \phi \cos^2 k}$ which vanishes for $k = \pi/2$ when $\Delta = 0$. In other words, the dynamics is completely insensitive to the gapless region generated by the identity term of (6).

The scaling of the defect density as given in Eq. (9) clearly satisfies the KZ scaling $n \sim \tau^{-\nu d/(\nu z + 1)}$, where d is the spatial dimensionality, with $d = z = \nu = 1$. However, we would like to highlight a subtle point here: when comparing with the conventional KZ scaling obtained for $\phi = 0$ [25], we observe that in the scaling (9), effectively

the parameter τ gets renormalized to $\tau_{\text{eff}} = \tau \cos^2 \phi$ as a consequence of the phase term in the hopping amplitude. The scaling of n as obtained via direct numerical integration of Eq. (7) is presented in Fig. 2 which indeed corroborates the analytical prediction.

The above study can be generalized to the non-linear quenching [36] of the form $\Delta = -1 + 2(t/\tau)^\alpha$, where t goes from 0 to τ , and $\alpha > 0$; the defect density has been found to satisfy a scaling relation $n \sim 1/(\cos \phi \tau^{\alpha/(\alpha+1)})$, where the result for the linear case is retrieved for $\alpha = 1$.

IV. QUENCHING DYNAMICS OF AN EDGE MAJORANA

Let us now focus on the dynamics of the above Majorana chain (5) under the quenching scheme $\Delta(t) = -1 + 2t/\tau$ along the path $\mu = 0$ (same quenching path as of the previous section). The non-linear time variation of the superconducting term also has been considered for the model in Eq. 5 (see Appendix B). Here, we start from an initial zero energy Majorana edge state with a real wavefunction $|\Psi(0)\rangle$ at $\Delta(0) = -1$ (i.e., in phase II) and investigate the possibility of its adiabatic transport to the other topological phase. By numerical integration of the time dependent Schrödinger equation we shall estimate following probabilities at the final instant $t = \tau$: probability of Majorana getting excited to the positive energy band P_{def} (negative energy band P_{neg})

$$P_{\text{def(neg)}} = \sum_{\epsilon^+ > 0 (\epsilon^- < 0)} |\langle \epsilon^+ (-) | \Psi(\tau) \rangle|^2, \quad (10)$$

where $|\epsilon^+ (-)\rangle$ corresponds to the positive and negative energy eigenstates of the final Hamiltonian within phase I with $\Delta = 1$ and $|\Psi(\tau)\rangle$ is the time-evolved Majorana state at $t = \tau$. We also calculate the modulus square of the overlap (P_m) between the final time-evolved state at $t = \tau$ and the zero energy equilibrium edge Majorana state with $\Delta = 1$ denoted by $|\epsilon_0\rangle$, defined as $P_m = |\langle \epsilon_0 | \Psi(\tau) \rangle|^2$. A non-zero value of this probability indicates a finite probability of finding an edge Majorana in phase I. Question remains what happens to P_m for $t > \tau$, when the final evolved state $|\Psi(\tau)\rangle$ evolves with the time-independent final Hamiltonian as $\exp(-iH(\Delta = 1)t)|\Psi(\tau)\rangle$. Noting that the $|\epsilon_0\rangle$ is an eigenstate (with zero energy) of the final Hamiltonian, it is straightforward to show that $P_m(t > \tau)$ calculated through $|\langle \epsilon_0 | \exp(-iH(\Delta = 1)t)|\Psi(\tau)\rangle|^2$ does not change with time which implies that there is always a finite probability of the edge Majorana in phase I for any $t > \tau$.

The variation of P_{def} and P_m as a function of τ for different values of ϕ with a system size $N = 100$ is shown in Fig. (3a) and Fig. (3b); clearly, there is no obvious scaling relation with τ as compared to the PBC scenario (see Sec. III). Interestingly, we find that although P_{def} remains fixed at 0.5 for small values of τ , there exists a characteristic τ (denoted by τ_c) for which the first significant dip in P_{def} occurs followed by a few drops. At

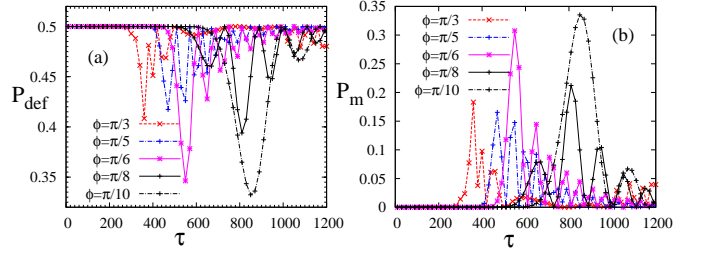


FIG. 3: (Color online) (a) The probability of defect (P_{def}) as a function of τ for different values of ϕ is being plotted which shows dip at different values of $\tau \geq \tau_c$ where the value of τ_c increases with decreasing ϕ . (b) The probability of Majorana (P_m) shows a peak exactly at those values of τ where P_{def} exhibits dips. Here, $N = 100$.

$\tau = \tau_c$, on the other hand, we find the first prominent peak (see Fig. (3b)) in P_m which implies a finite probability of an adiabatic tunneling of the initial edge Majorana following a quench from phase II to phase I. This can be contrasted to the case $\phi = 0$: P_m stays zero for all values of τ which means the adiabatic transport of the edge Majorana is completely forbidden and P_{def} is always equal to 1/2 implying that the edge Majorana gets completely delocalized within the bulk modes as reported in Ref. 25. Moreover, P_{def} and P_{neg} fall on top of each other signifying that evolved edge Majorana modes get delocalized within the same number of positive and negative energy interior bulk states with an equal probability for all values of τ (see Fig. (4a)).

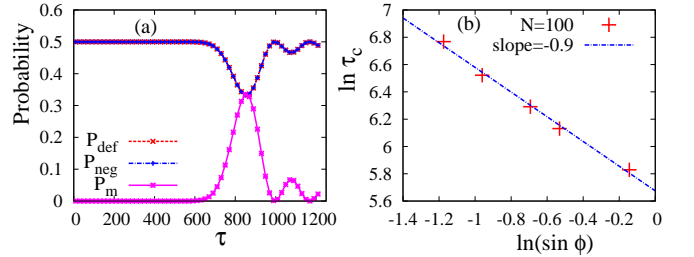


FIG. 4: (Color online) (a) Plots for P_{def} , P_{neg} and P_m with τ for $\phi = \pi/10$ show that all of them add upto unity. (b) The plot shows a linear variation of $\ln(\tau_c)$ as a function of $\ln(\sin \phi)$ with slope (≈ -0.9) nearly equal to -1.

Furthermore, analyzing the results presented in Figs. (3a, b), one can establish a relation between ϕ and τ_c which dictates the positions of the first significant dip (peak) in P_{def} (P_m). We observe that the value of τ_c increases with decreasing ϕ . Defining two instants of time when the system enters and leaves the gapless phase as t_e and t_o , respectively, the passage time through the gapless phase is found to be $\Delta t = t_o - t_e = \tau \sin \phi$. We observe that there exists an optimal value of Δt which is independent of ϕ (for a given N) when P_m becomes non-zero;

inspecting our numerical results, one can conclude that this optimal value is related to τ_c as

$$\Delta t_{\text{op}} = \tau_c \sin \phi. \quad (11)$$

It is noteworthy, that τ_c itself depends on ϕ and diverges when $\phi \rightarrow 0$, so that $P_m = 0$, for all values of τ suggesting the impossibility of an adiabatic transport of the edge Majorana in that case[25]. We plot $\ln \tau_c$ against $\ln \sin \phi$ in Fig. (4b) which establishes the relation between τ_c and $\sin \phi$ as given in Eq. (11) when Δt_{op} is fixed.

A close observation of Fig. (3a, b) suggests that there exists a set of relations of the same form like Eq. (11) for the passage times $\Delta t_{\text{op}1}, \Delta t_{\text{op}2}, \dots, \Delta t_{\text{op}n}$ ($\Delta t_{\text{op}(n-1)} < \Delta t_{\text{op}n}$) associated with the peaks in P_m ; where n is the number of peaks in P_m . The vanishing adiabatic transition probability P_m in the limit $\tau < \tau_c$, suggests the existence of a threshold value of transit time $\Delta t_{\text{th}} = \Delta t_{\text{op}1}$, which is a function of N , below of which the adiabatic tunneling of edge Majorana is forbidden. The variation of P_m , on the other hand, is shown as a function of τ for different values of system size with $\phi = \pi/5$ in Fig. 5(a). Fig. 5(b) shows that τ_c increases linearly with N for a fixed ϕ .

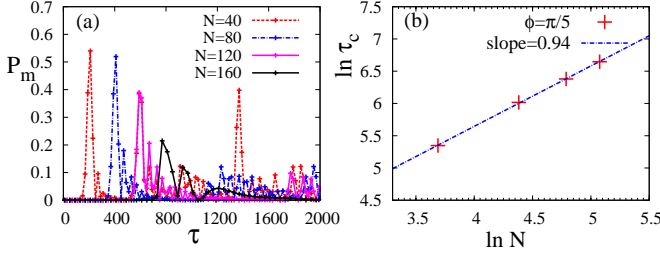


FIG. 5: (Color online) (a) Plots of P_m as a function of τ for different values of N with a fixed $\phi = \pi/5$. P_m shows peak at different values of $\tau \geq \tau_c$. (b) The figure shows a log-log plot between τ_c and N for the above ϕ with slope ($=0.94$) nearly equal to 1 confirming $\tau_c \sim N$.

We shall make a conjecture for the adiabatic transport of edge Majorana based on the following observations: the optimum transit time Δt_{op} governing the adiabatic passage, essentially depends only on the system size N whereas it marginally depends on the length of the quenching for the path $\mu = 0$, and the phase ϕ of the complex hopping term. We propose that for passage times of the order of (or greater than) Δt_{th} , the time evolved Majorana starts delocalizing only within the inverted energy levels (near zero energy) present inside the gapless region. For $\Delta t < \Delta t_{\text{th}}$, in contrary, the initial edge Majorana diffuses over all the interior positive and negative energy levels including the inverted levels (see Fig. (6)) prohibiting the possibility of an adiabatic transfer. The probability of getting an edge Majorana at the other phase after the quenching is maximum when

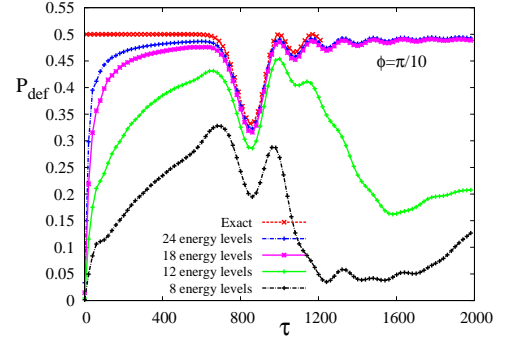


FIG. 6: (color online) The plot shows P_{def} as a function of τ considering overlaps between quenched Majorana state at final time and different number of positive bulk energy states (close to zero-energy) at the final parameter value. We consider the case $\phi = \pi/10$ and $N = 100$, where the number of inverted levels in both positive and negative sides of the zero energy level is 18 (see Appendix A). The plot signifies that in the limit of $\tau \leq \tau_c$ ($\Delta t < \Delta t_{\text{th}}$) the initial Majorana state interacts with all the energy levels. For the other regime, $\tau \geq \tau_c$, the P_{def} calculated using only the inverted positive energy levels nearly coincides with the exact P_{def} obtained considering all positive energy bands. This clearly confirms that time evolved Majorana states mix only with the inverted levels for a transit time $\Delta t \geq \Delta t_{\text{th}}$.

the time evolved Majorana state interacts with a minimal number of inverted bands so that the associated wave-function is closely related to the equilibrium wave-function of the edge Majorana at the other phase. This signature of efficiency in adiabatic tunneling is reflected in the Fig. (3b, 5a) where the first significant peak height of P_m decreases with increasing the number of inverted levels arising for larger N as well as ϕ .

In short, the conjecture is the following: in the limit of small τ , the Majorana gets delocalized over all the levels and hence there is no possibility of recombination after passage through the gapless phase. On the other hand, for finite τ (when τ is around τ_c and above that), the Majorana, in fact, gets delocalized only with the inverted region. Remarkably, there exists some optimal values of the passage time within the gapless phase for which the Majorana recombines partially from the inverted bands and one gets an adiabatic transfer to the other phase with a finite probability. Moreover, the adiabatic transport for an optimum transit time is more probable when the time evolved Majorana mixes with a minimal number of inverted bands.

Finally, the question remains why do τ_c and hence Δt_{op} increase with the system size as shown in Fig. (5b). The energy difference between two consecutive energy levels within the “inverted” region, decreases as N increases, leading to an increase in the characteristic relaxation time of the system and therefore a higher value of τ_c would be necessary for an adiabatic passage.

V. CONCLUSIONS

In summary, we discuss the quench dynamics of a modified version of a 1D p -wave superconducting chain by varying the superconducting gap term in a linear fashion in time. The quenching dynamics of the model with a PBC under the above quenching protocol, results in a defect density which is given by Kibble-Zurek scaling law with a modified quenching rate. On the other hand, we observe that there exist a finite probability of tunneling of an edge Majorana from one topological phase to the other at certain characteristic τ and ϕ , for an optimum transit time through the intermediate extended gapless region. We attribute the phenomenon of tunneling to the mixing of the time evolved Majorana states only with the inverted energy levels which is only possible above a threshold transit time that the system requires to cross the gapless region. Furthermore, there is a possible recombination of the Majorana state for some optimal values of the passage time. Interestingly, for an infinite system (in the thermodynamic limit), the threshold passage time Δt_{th} diverges and hence the adiabatic transport is impossible. On the other hand, for a periodic chain, the scaling of the defect density can be calculated exactly using the Landau-Zener transition formula and we find a Kibble-Zurek scaling with the quenching rate being renormalized by the phase term ϕ .

Acknowledgments

We sincerely thank Bikas K. Chakrabarti and Diptiman Sen for useful discussion regarding the work. AR thanks IIT Kanpur for providing hospitality during the part of this work. TN thanks SINP Kolkata for giving local hospitality during this work.

Appendix A: The spectrum with periodic, open boundary conditions and an irreducible coupling between a and b Majoranas

Here, we shall analyze the energy spectrum of the Hamiltonian (5) with periodic and open boundary conditions as shown in Fig. (7a) and Fig. (7b), respectively. The presence of two zero-energy lines in the spectrum of Hamiltonian with open boundary condition signifies that the phase I and II host two zero-energy Majorana modes at each end of the chain. In contrary, the system with periodic boundary condition does not have any edge Majorana mode. The diagram also shows that two inverted cones for both the positive and negative levels are present near zero energy. There is an inversion where the outer most bulk energy level, that becomes nearest to zero energy line at $\xi = -\sin \phi$, bends towards the interior bulk up to $\xi = 0$ without crossing the next energy level; after that it again bends in the opposite direction and becomes closest to the zero energy line at $\xi = \sin \phi$ above which

it again becomes the outer most bulk energy level. The range of ξ within which bending of energy levels occurs is decreasing as one moves away from the zero energy level towards the interior bands. As a result an inverted cone with vertex at $\xi = \Delta = 0$ appears at both side of the zero energy line. The inverted cones persist up to $\xi = \Delta = \pm \sin \phi$ (other two vertices of the cone). Cone like structures are also appearing deep inside (far away from zero energy) the positive and negative energy levels. The interior cone like structures are missing for $\phi = \pi/2$ as the inverted cones (both side of the zero energy) eat up that interior region. One can also see that the number of inverted levels increases with increasing N and ϕ (see Fig. 8).

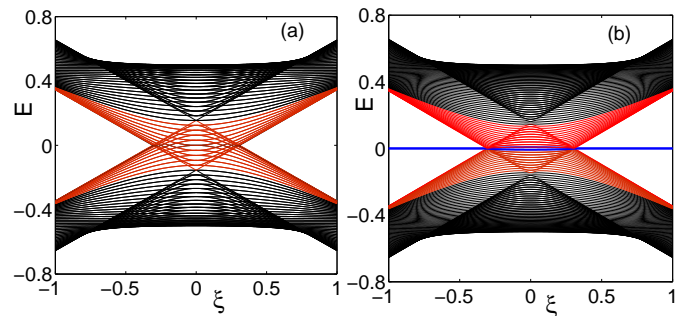


FIG. 7: (Color online) Plot shows the variation of energy levels as a function of parameter $\xi = \frac{\Delta}{w_0}$ (with $w_0 = 1$) for periodic (a) and open (b) boundary conditions with $\phi = \pi/10$ and $N = 100$.

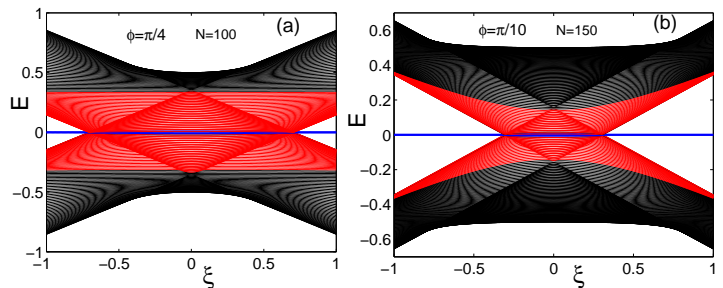


FIG. 8: (Color online) Plot shows the variation of energy levels as a function of parameter $\xi = \frac{\Delta}{w_0}$ (with $w_0 = 1$) for (a) $\phi = \pi/4$ and $N = 100$ and (b) $\phi = \pi/10$ and $N = 150$.

One can see that a and b Majorana particles are coupled to each other in an irreducible manner which is an outcome of the non-zero phase in the complex hopping term. The Heisenberg equations of motion for the zero-energy Majorana modes (a_n and b_n) using (5) are then

given by [7]

$$\begin{aligned}
i \dot{a}_n &= -[H, a_n] = 0, & i \dot{b}_n &= -[H, b_n] = 0, \\
w_0 \cos \phi (b_{n+1} + b_{n-1}) - \Delta (b_{n+1} - b_{n-1}) \\
&+ \mu b_n + w_0 \sin \phi (a_{n+1} - a_{n-1}) = 0, \\
w_0 \cos \phi (a_{n+1} + a_{n-1}) - \Delta (a_{n+1} - a_{n-1}) \\
&+ \mu a_n + w_0 \sin \phi (b_{n+1} - b_{n-1}) = 0. \quad (\text{A1})
\end{aligned}$$

By numerically diagonalizing the Hamiltonian (5), one can show that a_1 and b_1 are indeed coupled though the probability of a_1 is much higher than having a b_1 at the left edge of the chain if one chooses the same set of parameter values as given in the main text. An identical situation occurs at the right edge of the chain where both a_N and b_N exist with the probability of b_N being much higher than that of a_N . A topological invariant number which is different in two topological phases for this ETRS broken Hamiltonian has been introduced in the Ref. 7.

Appendix B: Adiabatic transport of edge Majorana in a power law quench

We generalize the quenching scheme to a non-linear quenching of the superconducting gap parameter using the protocol $\Delta = -1 + 2(t/\tau)^\alpha$ and then examine the adiabatic transport probability of edge Majorana with quench rate. Here as well, we find a finite tunneling probability of the edge Majoranas from phase II to phase I for a characteristic quench time τ_c which is a function of ϕ and the non-linearity α of the quenching scheme (see Fig. (9)). In fact, one can propose a scaling form $\Delta t = \sin \phi \tau^{2\alpha/\alpha+1} f(\tau/\tau_c)$ which has been constructed from a dimensionless combination of the hopping amplitude ($w_0 = 1$) and τ . Here we can see that as $\tau < \tau_c$, the scaling function $f(\tau/\tau_c) \sim \text{constant}$, implying $\Delta t < \Delta t_{\text{th}}$ which is in accordance with our results that the adiabatic transportation is forbidden below a threshold transit time. On the other limit, $\tau \geq \tau_c$, $f(\tau/\tau_c) \sim (\tau_c/\tau)^{2\alpha/\alpha+1}$. Optimal transit time looks like $\Delta t_{\text{op}} = \sin \phi \tau_c^{2\alpha/\alpha+1} \geq \Delta t_{\text{th}}$. As a result, P_m shows first significant peak at τ_c followed by a few peaks for $\tau > \tau_c$. The variation of τ_c with ϕ is shown in Fig. (9) which closely matches with this predicted scaling form. Therefore, we can say that the possibility of adiabatic transport of edge Majoranas for this model shows up even for a non-linear quenching.

Appendix C: Signature of localization of Majorana

In this section, we analyze the Hamiltonian with PBC (given in Eq. (6)) further. We consider the LZ part of the Hamiltonian which can be written as

$$h_k^{LZ} = \xi_k s^z + \delta_k s^y, \quad (\text{C1})$$

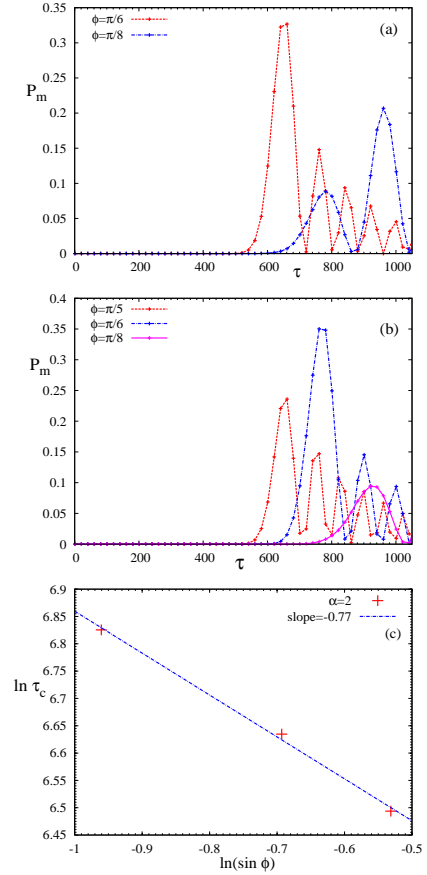


FIG. 9: (Color online) (a) Plots of P_m for a non-linear time variation with $\alpha = 1.5$ as a function of τ with different values of ϕ . (b) Plots of P_m as a function of τ for different values of ϕ with $\alpha = 2$. (c) The plot shows a linear variation of $\ln \tau_c$ as a function of $\ln \sin \phi$ with slope (≈ -0.77) nearly equal to -0.75 for $\alpha = 2$. It justifies that τ_c is proportional to $\sin \phi^{-(\alpha+1)/2\alpha}$ for a fixed Δt_{op} . Here $N = 100$.

with $\xi_k = 2\Delta \sin k$ and $\delta_k = 2\cos \phi \cos k$. The above Hamiltonian can be expressed in terms of the Bogoliubov operators which reduces the Hamiltonian to a diagonal one. The transformation relations are given by

$$\begin{aligned}
b_k &= u_k f_k - i v_k f_{-k}^\dagger, \\
b_{-k} &= u_k f_{-k} + i v_k f_k^\dagger,
\end{aligned} \quad (\text{C2})$$

where b_k and b_{-k} are Bogoliubov fermionic operators which satisfy the anti-commutation relations. The parameters (u_k and v_k) satisfy the relation $|u_k|^2 + |v_k|^2 = 1$ for each k -mode and are defined as

$$u_k = \frac{1}{\sqrt{2}} \sqrt{1 + \frac{\xi_k}{\varepsilon_k}}, \quad v_k = \frac{1}{\sqrt{2}} \sqrt{1 - \frac{\xi_k}{\varepsilon_k}} \quad (\text{C3})$$

where $\varepsilon_k = \sqrt{\xi_k^2 + \delta_k^2}$. Finally, the Hamiltonian (2) of the main text can be written in term of the Bogoliubov

fermions as

$$H = \sum_{k>0} \varepsilon_k b_k^\dagger b_k \quad (\text{C4})$$

For $\phi = 0$, the values of u_k and v_k are the same ($= 1/\sqrt{2}$) at the critical point ($\Delta = 0$). The equilibrium edge Majorana states at the critical point can be cast only by an equal superposition of positive and negative energy bulk excitations associated with the $k_c = \pm\pi/2$ over the Bogoliubov vacuum. As a consequence of that the edge Majorana gets equally delocalized throughout the chain in real space as soon as system crosses the gapless critical line separating two topological phases [25].

For $\phi \neq 0$, on the other hand, there is an extended gapless region bounded by two horizontal lines $\Delta = \pm \sin \phi$ (see the phase diagram). Within the gapless phase,

$u_k \neq v_k$, for any $\Delta \neq 0$ while they are only equal when $\Delta = 0$. Therefore, we have a large number of Bogoliubov operators (given in Eq. (C2)) associated with the critical modes ($\pi/2 - \phi$ to $\pi/2 + \phi$ and $-\pi/2 - \phi$ to $-\pi/2 + \phi$) within the gapless region. Consequently, in the momentum space the system is not highly localized near only two bulk gapless critical modes as happens for the case of $\phi = 0$. The equilibrium edge Majorana states can not be written by an unequal superposition of positive and negative energy bulk excitation associated with the critical momentum modes present inside the gapless region for any non-zero Δ . This implies that the edge Majoranas do not delocalize uniformly throughout the chain when the system crosses the extended gapless quantum critical region separating two topological phases.

-
- [1] A. Kitaev, Physics-Uspekhi **44**, 131 (2001), arXiv:cond-mat/0010440v2 (2000).
 - [2] I. C. Fulga, F. Hassler, A. R. Akhmerov, and C. W. J. Beenakker, Phys. Rev. B **83**, 155429 (2011).
 - [3] J. D. Sau and S. Das Sarma, Nature communications **3**, 964 (2012).
 - [4] R. M. Lutchyn and M. P. A. Fisher, Phys. Rev. B **84**, 214528 (2011).
 - [5] W. DeGottardi, D. Sen, and S. Vishveshwara, New J. Phys. **13**, 065028 (2011).
 - [6] W. DeGottardi, D. Sen, and S. Vishveshwara, Phys. Rev. Lett. **110**, 146404 (2013).
 - [7] W. DeGottardi, M. Thakurathi, S. Vishveshwara, and D. Sen, Phys. Rev. B **88**, 165111 (2013).
 - [8] A. Kitaev and C. Laumann, arXiv:0904.2771v1 (2009).
 - [9] J. C. Budich, S. Walter and B. Tranzettel, Phys. Rev. B **85**, 121405 (R) 2012.
 - [10] M. J. Schmidt, D. Rainis and D. Loss, Phys. Rev. B **86**, 085414 (2012).
 - [11] M. Z. Hasan and C.L. Kane, Rev. Mod. Phys. **82**, 3045 (2010).
 - [12] X.-L. Qi and S.-C. Zhang, Rev. Mod. Phys. **83**, 1057 (2011).
 - [13] L. Fu and C.L. Kane, Phys. Rev. Lett. **100**, 096407 (2008).
 - [14] V. Mourik et al., Science **336**, 1003 (2012).
 - [15] M.T. Deng, C.L. Yu, G.Y. Huang, M. Larsson, P. Caroff, and H.Q. Xu, Nano Lett. **12**, 6414 (2012).
 - [16] A. Das, Y. Ronen, Y. Most, Y. Oreg, M. Heiblum, and H. Shtrikman, Nat. Phys. **8**, 887 (2012).
 - [17] W. Chang, V. Manucharyan, T. Jespersen, J. Nygard, and C. Marcus, Phys. Rev. Lett. **110**, 217005 (2013).
 - [18] E. J. H. Lee, X. Jiang, M. Houzet, R. Aguado, C. M. Lieber, and S. De Franceschi, Nature Nanotechnol **9**, 79-84 (2014).
 - [19] D. Rainis, L. Trifunovic, J. Klinovaja, and D. Loss, Phys. Rev. B, **87**, 024515 (2013).
 - [20] A. D. K. Finck, D. J. Van Harlingen, P. K. Mohseni, K. Jung, and X. Li, Phys. Rev. Lett. **110**, 126406 (2013).
 - [21] J. Dziarmaga, Adv. Phys. **59**, 1063 (2010).
 - [22] A. Polkovnikov, K. Sengupta, A. Silva, and M. Vengalattore, Rev. Mod. Phys. **83**, 863 (2011).
 - [23] A. Dutta, U. Divakaran, D. Sen, B.K. Chakrabarti, T.F. Rosenbaum, and G. Aeppli, arXiv:1012.0653v2 (2010).
 - [24] A. Bermudez, D. Patan, L. Amico, M. A. Martin-Delgado, Phys. Rev. Lett. **102**, 135702 (2009).
 - [25] A. Bermudez, L. Amico, and M.A. Martin-Delgado, New J. Phys. **12**, 055014 (2010).
 - [26] P. Wang, W. Yi, and G. Xianlong, arXiv: 1404.6848v1 (2014).
 - [27] A.A. Patel, S. Sharma, and A. Dutta, Eur. Phys. J. B **86**, 367 (2013).
 - [28] A. Rajak and A. Dutta, Phys. Rev. E **89**, 042125 (2014).
 - [29] M.-C. Chung, Y. -H. Jhu, P. Chen, C.-Y. Mou, and X. Wan, arXiv:1401.0433.
 - [30] P.D. Sacramento, arXiv: 1404.5141v1.
 - [31] M. Thakurathi, A.A. Patel, D. Sen, and A. Dutta, Phys. Rev. B **88**, 155133 (2013).
 - [32] E. Perfetto, Phys. Rev. Lett. **110**, 087001 (2013).
 - [33] D. Chowdhury, U. Divakaran, and A. Dutta, Phys. rev. E **81** 012101 (2010).
 - [34] C. Zener, Proc. R. Soc. London, Ser. A **137**, 696 (1932); L.D. Landau and E. M. Lifshitz, *Quantum Mechanics: Non-relativistic Theory*, 2nd ed. Pergamon, Oxford, 1965.
 - [35] S. Suzuki and M. Okada, in Quantum Annealing and Related Optimization Methods, Ed. by A. Das and B. K. Chakrabarti (Springer-Verlag, Berlin, 2005).
 - [36] D. Sen, K. Sengupta, and S. Mondal, phys. Rev. Lett **101** 016806 (2008), W. De Grandi, R. A. Barankov, and A. Polkovnikov, Phys. Rev. Lett **101** 230402 (2008).